Journal of Loss Prevention in the Process Industries 63 (2020) 103999

Contents lists available at ScienceDirect

Journal of Loss Prevention in the Process Industries

journal homepage: http://www.elsevier.com/locate/jlp

Computational fluid dynamics simulations of hydrogen releases and vented deflagrations in large enclosures

Melodía Lucas [a,*], Trygve Skjold [b], Helene Hisken [a]

[a] Gexcon, Fantoftvegen 38, 5072, Bergen, Norway
[b] University of Bergen, Allégaten 55, 5007, Bergen, Norway

ARTICLE INFO

Keywords:
Hydrogen safety
Inhomogeneous mixtures
Stratified mixtures
Large enclosures
Vented hydrogen deflagrations
Computational fluid dynamics

ABSTRACT

This paper presents model predictions obtained with the CFD tool FLACS for hydrogen releases and vented deflagrations in containers and larger enclosures. The paper consists of two parts. The first part compares experimental results and model predictions for two test cases: experiments performed by Gexcon in 20-foot ISO containers (volume 33 m^3) as part of the HySEA project and experiments conducted by SRI International and Sandia National Laboratories in a scaled warehouse geometry (volume 45.4 m^3). The second part explores the use of the model system validated in the first part to accidental releases of hydrogen from forklift trucks inside a full-scale warehouse geometry (32 400 m^3). The results demonstrate the importance of using realistic and reasonably accurate geometry models of the systems under consideration when performing CFD-based risk assessment studies. The discussion highlights the significant inherent uncertainty associated with quantitative risk assessments for vented hydrogen deflagrations in complex geometries. The suggestions for further work include a pragmatic approach for developing empirical correlations for pressure loads from vented hydrogen deflagrations in industrial warehouses with hydrogen-powered forklift trucks.

1. Introduction

Policy changes in response to the United Nations (UN) sustainable development goals (SDGs) have resulted in an increased focus on the use of hydrogen as an energy carrier (UN, 2018). One relevant example is the replacement of batteries by hydrogen fuel cells for powering forklift trucks in warehouses (Ekoto et al., 2012; Houf et al., 2012; Bauwens and Dorofeev, 2014). Accidental releases of hydrogen in confined geometries will typically result in stratified mixtures (Hooker et al., 2017; Skjold et al., 2019a). For a given mass of released hydrogen, rapid combustion of the reactive parts of a stratified fuel-air cloud may produce significantly higher overpressures than flame propagation through a lean, less reactive homogeneous mixture that occupies the entire enclosure (Makarov et al., 2018; Skjold et al., 2019a). Furthermore, the pressure loads may increase significantly if the flammable cloud occupies a region with congestion and/or partial confinement.

The primary means of mitigating the consequences of deflagrations inside process vessels, containers and buildings entail the use of explosion venting devices. However, the European standard for the design of gas explosion venting protective systems is not valid for hydrogen systems and does not account for congestion inside the enclosure (EN 14994, 2007). To address this limitation, the European Commission (EC) and the Fuel Cells and Hydrogen Joint Undertaking (FCH JU) supported the project *Improving Hydrogen Safety for Energy Applications through pre-normative research on vented deflagrations* (HySEA). The primary objective of the HySEA project was to develop recommendations for improved international standards, such as EN 14994 (2007) and NFPA 68 (2018). The project included full-scale vented explosion experiments in 20-foot ISO containers (Skjold, 2018a, Skjold, 2018b; Skjold et al., 2019b) and smaller enclosures (Carcassi et al., 2018; Schiavetti et al., 2019), as well as various approaches to the modelling of vented hydrogen deflagrations (Sinha et al., 2019a, 2019b; Sinha and Wen, 2019; Rao and Wen, 2019; Lakshmipathy et al., 2019; Pini et al., 2019; Atanga et al., 2019). This paper presents results obtained with the computational fluid dynamics (CFD) tool FLACS-Hydrogen for scenarios involving release and dispersion of hydrogen, followed by vented deflagrations, in enclosures at different spatial scales. The model results include two validation studies and a study of realistic accident scenarios in a hypothetical full-scale warehouse geometry. The discussion elaborates on the implications of the results for quantitative risk assessments (QRAs) for warehouses that apply hydrogen-powered forklift trucks, including suggestions for further work.

* Corresponding author.
E-mail address: melodia@gexcon.com (M. Lucas).

https://doi.org/10.1016/j.jlp.2019.103999
Received 18 June 2019; Received in revised form 30 September 2019; Accepted 4 November 2019
Available online 9 November 2019

2. FLACS-Hydrogen

The CFD tool FLACS is used for engineering calculations related to process safety applications, such as consequence modelling for various accident scenarios in industrial facilities (Gexcon, 2019). The numerical solver in FLACS uses the SIMPLE algorithm (Patankar and Spalding, 1972), extended to handle compressible flows (Hjertager, 1982), and a first-order backward Euler temporal scheme for solving the Reynolds-averaged Navier-Stokes (RANS) equations on a structured Cartesian grid. FLACS belongs to the porosity/distributed resistance (PDR) family of CFD solvers. Turbulent premixed combustion is modelled by a standard two-equation turbulence model with added sub-grid contributions for turbulence generation, together with transport equations for the fuel mass fraction and a fuel-air mixture fraction. The combustion model accounts for the increase in burning velocity due to turbulence and flame folding due to sub-grid objects. Since the sub-grid models for turbulence and combustion are formulated to give reasonable results on a relatively coarse grid, the model predictions do not necessarily converge for gradual refinement of the computational mesh. Users of the software must therefore follow grid guidelines derived from validation studies.

The preparation for a new release of FLACS entails extensive validation against experimental data and systematic optimisation of selected parameters in the model system (Both, 2019). FLACS-Hydrogen is a subversion of FLACS developed for hydrogen energy applications. The initial development of FLACS-Hydrogen took place in connection with the Network of Excellence (NoE) HySafe funded by the European Commission (Middha, 2010). This paper presents simulations performed with the latest version of FLACS-Hydrogen (*v10.9*). Previous publications describe the dispersion and combustion models in FLACS in more detail (Hisken, 2018; Lucas et al., 2019), as well as inherent limitations in the modelling of physical phenomena related to dispersion and combustion of hydrogen (Skjold et al., 2019a).

3. Validation cases

This section describes model validation for two test cases that are relevant for accident scenarios in warehouses that apply hydrogen-powered forklift trucks: experiments performed by Gexcon in 20-foot ISO containers and experiments conducted by SRI International and Sandia National Laboratories in a scaled warehouse geometry.

3.1. Experiments in 20-foot containers

Skjold et al., 2019b summarise the experimental configurations and the overall results for the 66 vented deflagration tests in 20-foot containers that Gexcon performed as part of the HySEA project. The experimental rig consisted of a 20-foot ISO container with a steel frame on the floor for mounting pressure transducers and various obstacle configurations. The test configurations described in this paper involved either an empty container with only the frame inserted (FO), or a pipe rack installed in centre position inside the container (P2).

Table 1 summarises the test matrix and the maximum reduced explosion pressures P_{max} from the 22 tests that involved stratified mixtures, including five unignited tests (39–43). The range of values for P_{max} quantifies the uncertainty resulting from applying digital smoothing filters, with frequencies 33, 50 and 100 Hz (Skjold, 2018a, Skjold, 2018b; Skjold et al., 2019b). The measurement error for the piezoelectric pressure sensors is less than ±1% of full-scale output, which is negligible compared to the inherent uncertainty associated with temperature drift, post-processing and the inherent spread in results between repeated tests (Skjold et al., 2019a).

The nominal hydrogen concentrations $C_{H2,nom}$ in Table 1 indicate the concentration that would result with perfect mixing and negligible loss of hydrogen from the container. Hydrogen was released inside the containers at a constant flow rate, either from a circular pipe with inner diameter 18 mm or from a cubical box. The box contained porous material and the flow exited through a perforated plate to imitate a diffusive area leak with dimensions 0.20 m × 0.20 m. The releases were positioned in the middle of the container, 0.30 m above the floor and pointing upwards. The releases had a duration of 450 s (7.5 min). A closer examination of the measured mass flow rates and release durations resulted in a few corrections to the nominal concentrations listed in Table 1, relative to previous publications (Skjold et al., 2019a). The

Table 1
Summary of experiments in 20-foot containers with stratified mixtures.

Test	Nozzle	Flow rate ($Nm^3\ hr^{-1}$)	t_{leak} (s)	t_{ign} (s)	$C_{H2,nom}$ (vol%)	A_v (m^2)	Vent	Obst.	P_{max} (bar)
39	Jet	56	450	n/a	21	n/a	n/a	P2	n/a
40	Diff.	56	450	n/a	21	n/a	n/a	P2	n/a
41	Diff.	56	450	n/a	21	n/a	n/a	FO	n/a
42	Jet	56	450	n/a	21	n/a	n/a	FO	n/a
43	Jet	56	450	n/a	21	n/a	n/a	FO	n/a
44	Diff.	56	450	480	21	6	P	FO	0.391–0.436
49	Diff.	42	450	480	15	6	P	P2	0.177–0.188
50	Jet	42	450	480	15	6	P	P2	0.189–0.195
51	Jet	42	450	480	15	6	O	P2	0.061–0.063
52	Diff.	42	450	480	15	6	O	P2	0.069–0.079
53	Diff.	42	450	480	15	6	O	FO	0.102–0.114
54	Jet	42	450	480	15	6	O	FO	0.072–0.082
55	Jet	42 [c]	450	485	14–15	6	P	FO	0.154–0.163
56	Diff.	42 [c]	450	480	14–15	6	P	FO	0.158–0.166
57 [a]	Jet	56 [c]	450	480	20–21	6	P	FO	0.314–0.343
59 [a]	Jet	56 [c]	450	480	20–21	6	P	FO	0.319–0.342
60 [a]	Jet	56	450	480	21	6	P	P2	0.344–0.370
61 [a]	Jet	56	450	480	21	6	P	P2	0.514–0.677
62	Jet	40	450	480	15	6	P	P2	0.151–0.158
63	Diff.	40 [d]	345	405	≈10	5 [b]	P	P2	0.170–0.173
64	Diff.	40	450	480	15	6	P	FO	0.152–0.162
65	Jet	40	450	480	15	6	P	FO	0.158–0.163

[a] The second HySEA blind-prediction benchmark exercise involved tests 57, 59, 60 and 61 (Skjold et al., 2019a).

[b] Only five of the six vent panels installed on the container opened in test 63 (Skjold et al., 2019b).

[c] Due to low temperatures, the actual flow rates for tests 55 (Fig. 1), 56 (Fig. 3), 57 and 59 (Skjold et al., 2019a) was probably about 3 $Nm^3\ hr^{-1}$ lower than the target values indicated in Table 1.

[d] The specified release rate of 40 $Nm^3\ hr^{-1}$ could not be maintained for the intended duration in test 63 because the hydrogen cylinder was empty before the test ended.

range of values for tests 55, 56, 57 and 59 indicates uncertainty in the flow measurements due to low temperature during testing. Fig. 1 and Fig. 2, as well as previous work reported by Skjold et al., 2019a, summarise the volumetric flow rate and duration of the hydrogen releases.

Hydrogen concentrations were measured at various heights with both low-cost oxygen sensors from Teledyne instruments (continuous measurements, estimated accuracy ± 0.6 vol%) and a Servomex Xendos 2223 oxygen transmitter/analyser (estimated accuracy ± 0.2 vol%). The latter technique involved intermittent measurements, where the same instrument analysed gas sampled from different positions (Skjold et al., 2019a). The measurement points were located in opposite corners of the container, 2.2, 1.8, 1.4, 1.0 and 0.6 m above the floor, for sensors A4-A4′, B4-B4′, C4-C4′, D4-D4′ and E4-E4′, respectively. The symmetric location of the vertical row of concentration probes (A4, B4, etc.) and sampling tubes (A4′, B4', etc.) implies that the continuous and intermittent concentration measurements should measure similar concentration profiles for the stratified mixtures inside the container.

The stratified hydrogen-air mixtures were ignited 2 m above the floor of the container, 30 s after the release stopped (Skjold et al., 2019a). The explosions were vented through six 1.0 m × 1.0 m vent openings on the roof of the container, covered with single-sheet bulged vent panels. The total vent area A_v was 6.0 m^2, P_{stat} was 100 ± 25 mbar, and the specific weight of the panels was 6.8 kg m^{-2}.

3.1.1. Simulations

Tests 39, 42–43, 57 and 59–61 with jet releases from a pipe were part of the second HySEA blind-prediction benchmark study, which included predictions with previous versions of FLACS-Hydrogen (Skjold et al., 2019a). The CFD simulations presented here include additional diffusive area releases from the porous box. The simulations use 10 cm cubical grid cells within the container and grid refinement at the leak points according to the user guidelines (Gexcon, 2019). The releases from the pipe were modelled as a jet leak, and the releases from the box were modelled as a diffuse leak. For the jet releases, the grid was refined to match the area of the release, and the CFLC number was increased to 125 to reduce the effect of the local grid refinement on the time steps. The diffusive releases were resolved with four computational cells, and the CFLC number was set to 80. The CPU-times for these simulations were about 136 h for the jet releases and 25 h for the diffusive releases.

3.1.2. Results and discussion

Fig. 3 compares experimental and simulated hydrogen concentrations at each sensor location for 42 Nm^3 h^{-1} diffusive releases with an empty container (tests 53 and 56 on the right) and a container with the pipe rack in centre position (tests 49 and 52 on the left). The simulations predict the stratification inside the container with reasonable accuracy. Fig. 4 compares experimental results to simulations at each sensor location for 42 Nm^3 h^{-1} jet releases with an empty container (tests 55 and 54 on the left) and a container with the pipe rack in centre position (tests 50 and 51 on the right). There is reasonable agreement between experiments and simulations for monitor points A4, B4, C4 and D4. However, for the jet releases, the simulated concentration at monitor point E4 increases sooner and is about five volume per cent higher than the experimental values. Higher grid resolution and shorter time steps may reduce the numerical diffusion, and hence yield more accurate results, at the expense of a considerable increase in CPU-hours.

Fig. 5 compares experimental and simulated hydrogen concentrations for test 64, with a 40 Nm^3 h^{-1} diffusive release in the empty container. Fig. 6 compares results for the 40 Nm^3 h^{-1} jet releases in tests 65 and 62, with empty container (FO) and pipe rack (P2), respectively. The intermittent concentration measurements were not available for some of these tests. The increase in hydrogen concentration occurs sooner in the simulations compared to the experiments, but the slopes of the concentration curves are similar.

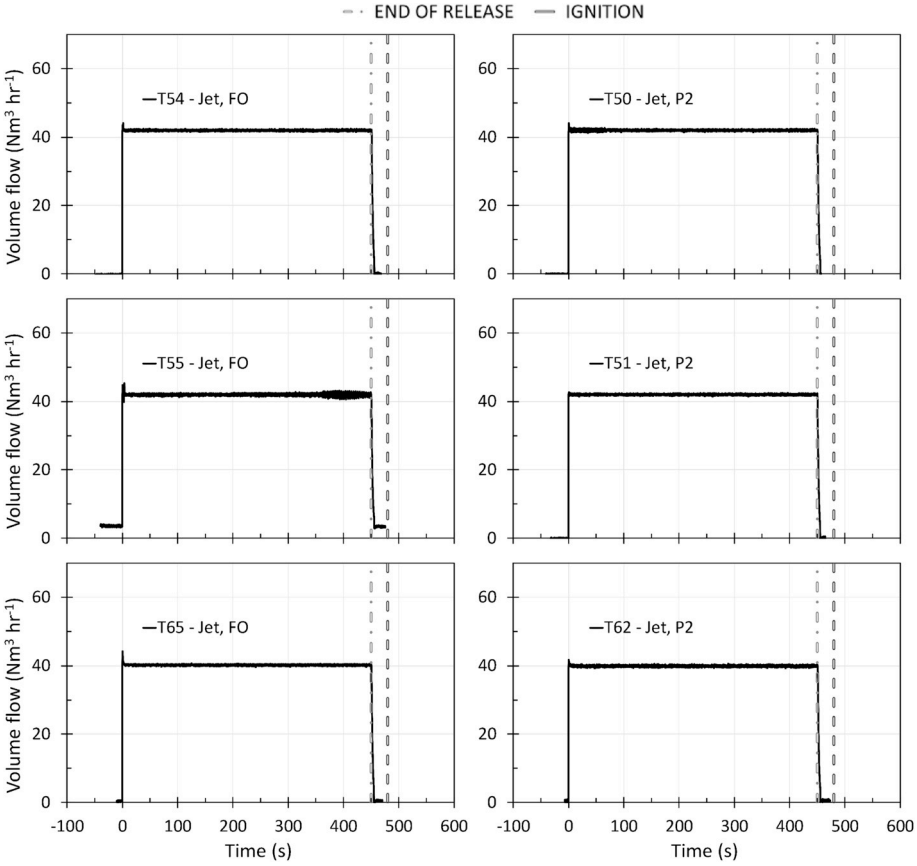

Fig. 1. Measured flow rates for jet releases in empty containers (FO) and in containers with pipe rack (P2).

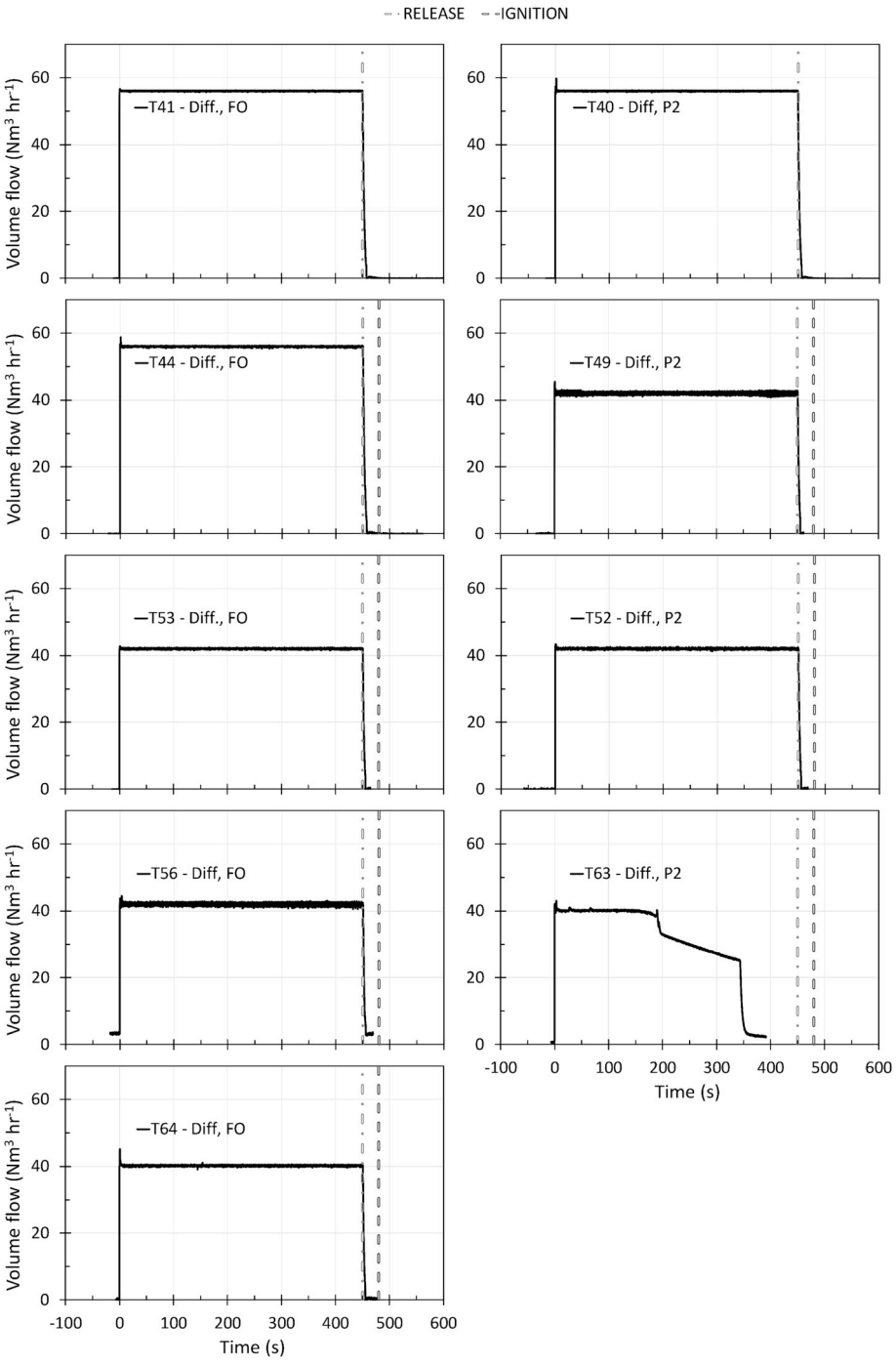

Fig. 2. Measured flow rates for diffusive area releases in empty containers (FO) and in containers with pipe rack (P2).

Fig. 7 compares measured and simulated concentration profiles 450 s after onset of 56 $Nm^3\ h^{-1}$ jet (tests 59, 57 and 42) and diffusive (tests 44 and 41) releases in empty container (FO). The two release modes result in similar stratification inside the container, but the CFD simulations predict less pronounced stratification for the jet release. Fig. 8 compares measured and simulated concentration profiles 450 s after onset of 42 $m^3\ h^{-1}$ jet (tests 50 and 51) and diffusive (test 53 and 56) releases in a container with the pipe rack obstacle in the centre position (P2). The presence of the obstacle has negligible influence on the stratification inside the container. Fig. 9 illustrates the simulated stratification of hydrogen after 450 s in a vertical cross-section for four release scenarios: diffusive (D) and jet (J) releases, with (P2) and without (FO) the pipe rack obstacle.

There is reasonable agreement between the experimental results and the CFD simulations, given the uncertainty in the measurements and the inherent variation in results from repeated tests. This observation is consistent with the results from the second blind-prediction benchmark study in the HySEA project (Skjold et al., 2019a). However, the blind-prediction study also revealed that results from CFD simulations can vary significantly, for different codes as well as for different users of the same software.

3.2. *Experiments in a scaled warehouse geometry*

Ekoto et al. (2012) described a series of experiments with hydrogen releases performed by SRI International and Sandia National

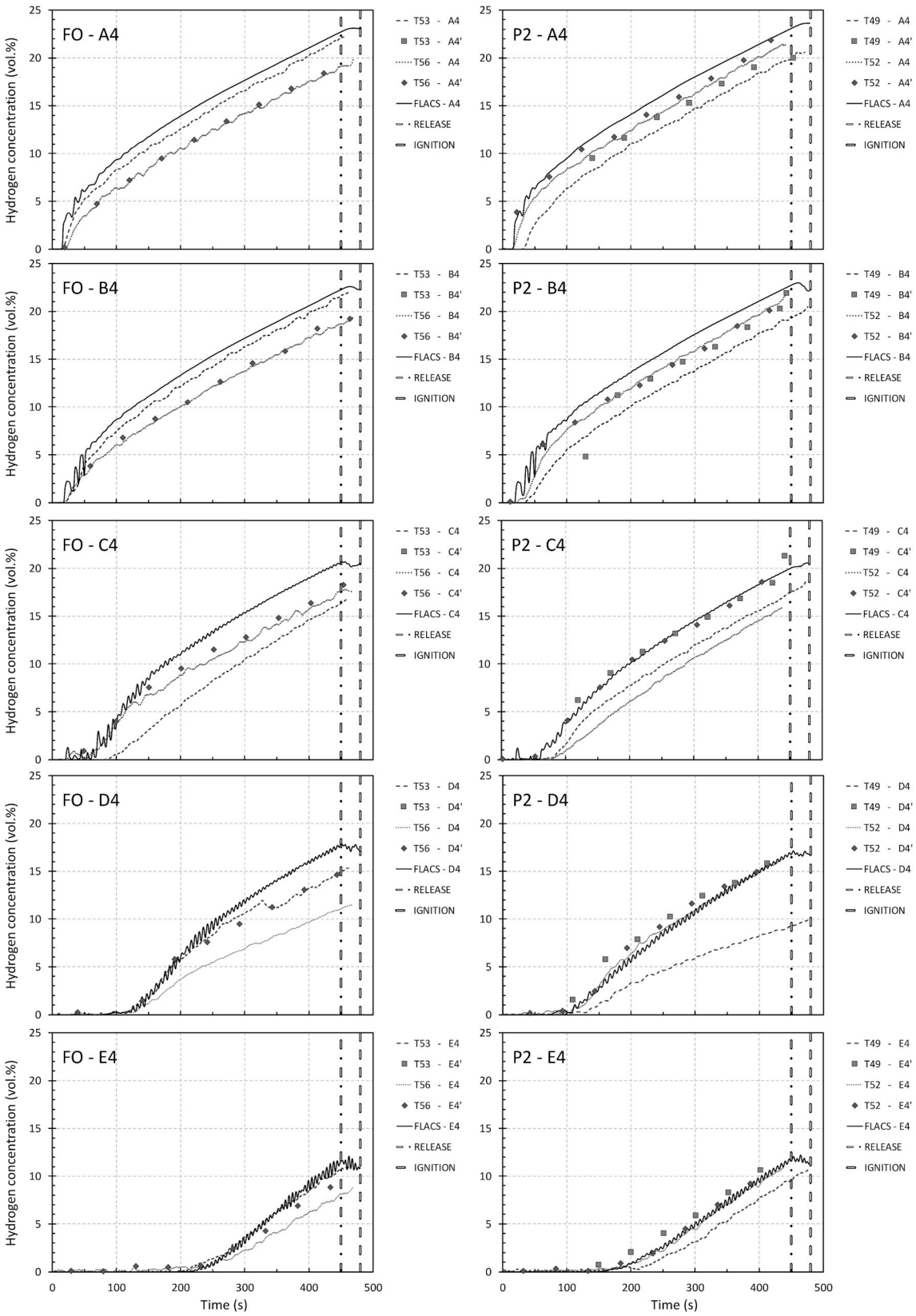

Fig. 3. Measured (dotted lines) and simulated (solid lines) hydrogen concentrations for 42 Nm^3h^{-1} diffusive releases with empty container (FO) and container with pipe rack in centre position (P2). The continuous measurements for test 53 were not available.

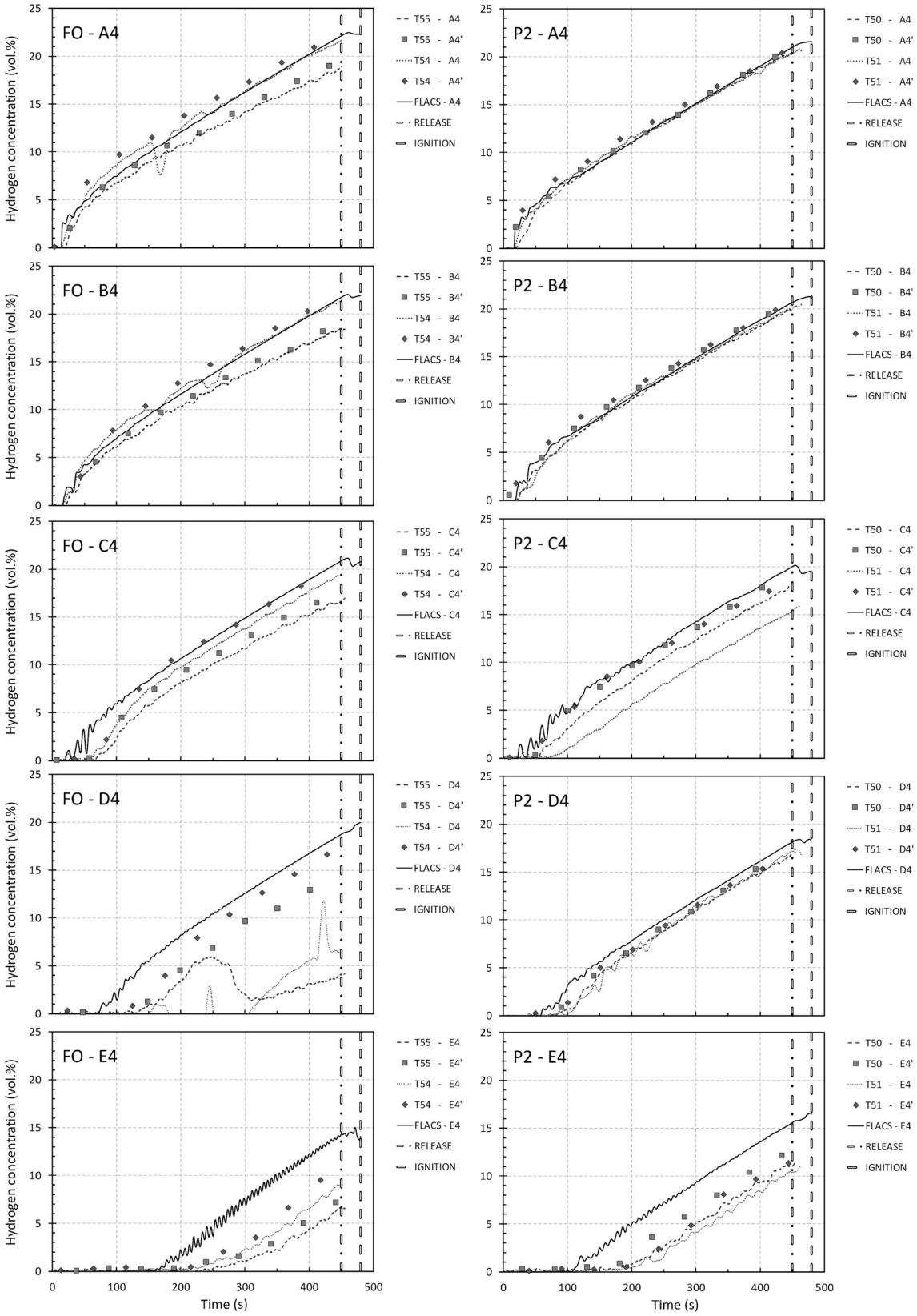

Fig. 4. Measured (dotted lines) and simulated (solid lines) hydrogen concentrations for 42 Nm^3h^{-1} jet releases with frame only (FO) and with the pipe rack in centre position (P2).

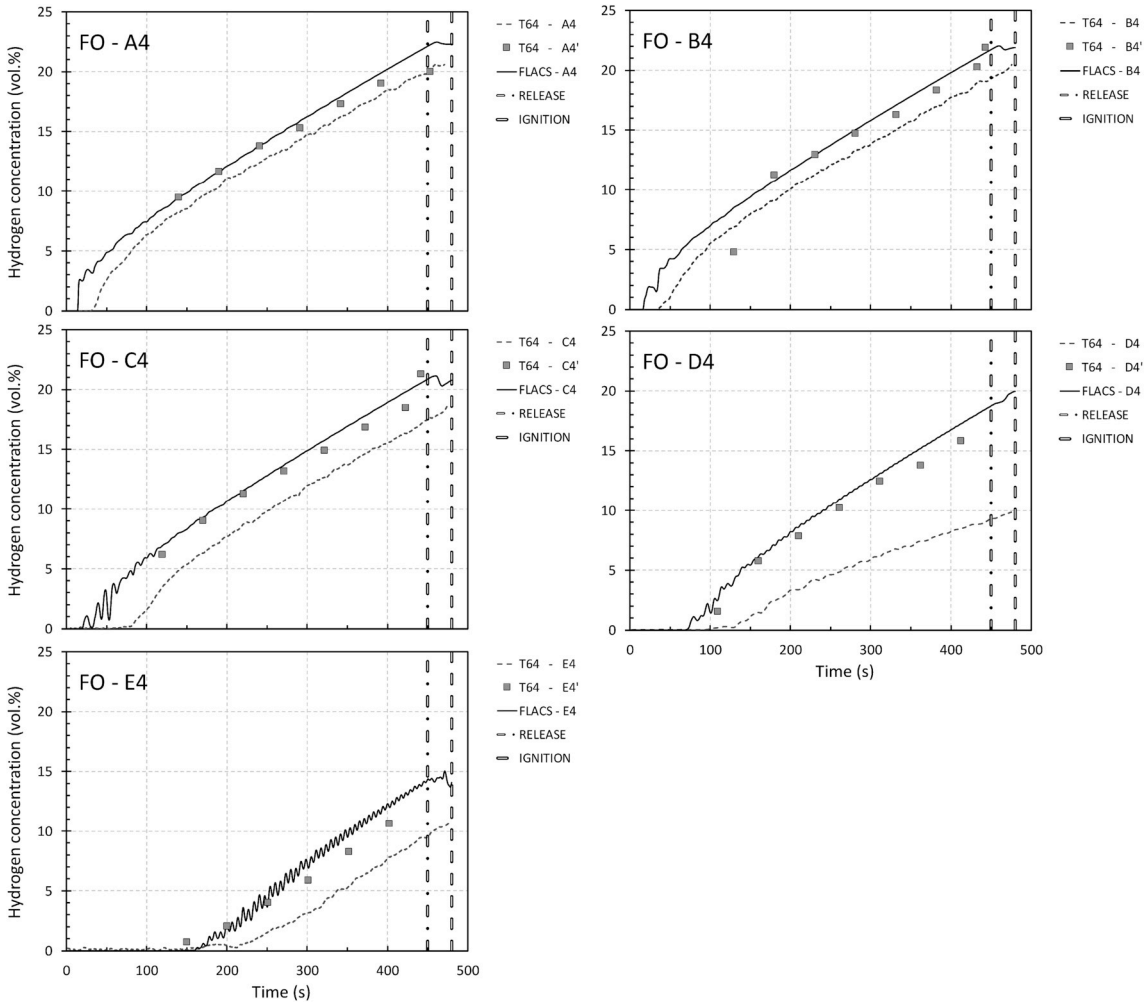

Fig. 5. Measured (dotted lines) and simulated (solid lines) hydrogen concentrations for a 40 Nm^3h^{-1} diffusive release with the pipe rack in centre position (P2).

Laboratories in a 45.4 m^3 scaled warehouse facility at the SRI Corral Hollow Experimental Site (CHES) in Livermore, California. The test series included three unignited and ten ignited releases. Table 2 shows the tests performed without forced convection that were selected for validation of FLACS. The specification of the release scenarios was based on information from manufacturers of forklift trucks and normalised Froude scaling for relevant parameters. Houf et al. (2012) found good agreement between the experimental results reported by Ekoto et al. (2012) and CFD simulations. They used the FUEGO solver developed by Sandia to simulate the release and dispersion scenarios and FLACS-Hydrogen *v9.1* to simulate the deflagrations. Bauwens and Dorofeev (2014) modelled the release scenarios with FireFOAM and estimated the peak overpressure from the total mass of hydrogen above the lower flammability limit inside the enclosure.

3.2.1. Simulations

Fig. 10 illustrates the geometry model and computational mesh used for the simulations with FLACS-Hydrogen *v10.9*. The source term for the release and dispersion simulations was an area leak with time-dependent flow rate specified in a leak file (cl-file) according to the modelling of blowdown of a 3.63-L tank with initial pressure 13.45 MPa through a 3.56 mm orifice (Ekoto et al., 2012). The computational grid near the leak was refined according to guidelines, using 2×2 computational cells to resolve the diffusive leak. The grid for the vented deflagration simulations was stretched in all directions outside the enclosure. In the simulations, the vent opening was initially covered by pop-out panels with specific mass 6.9 $kg\,m^{-2}$ and static opening pressures taken from the experiments by Ekoto et al.

3.2.2. Results and discussion

Fig. 11 summarises the results from the dispersion simulations with FLACS-Hydrogen *v10.9* for two repeated experiments and two grid resolutions. Sensors S01, S06 and S08 were located near the release point, and sensors S04, S07 and S11 were located in the ceiling (Ekoto et al., 2012). The simulations capture the stratification observed in the experiments reasonably well for both grid resolutions (see Fig. 11).

The simulations of vented deflagrations used the flow and concentration fields from the dispersion simulations as initial conditions. Fig. 12 and Fig. 13 compare experimental and simulated pressure-time histories at the sidewall closest to the release and 1.3 m above ground. Fig. 12 shows that the simulations capture the effect of varying the strength of the pressure relief panels. Fig. 13 shows results for the tests with fully reinforced vent openings and ignition either near the forklift (I1) or near the ceiling (I2), with ignition delays 3.0 and 3.5 s from onset of release, respectively. Compared to simulations, the experiments show a more pronounced reduction in overpressure for ignition near the ceiling, relative to ignition near the forklift. A plausible explanation can be that the flammability limits in the model do not differentiate between upwards and downwards flame propagation. Another source of uncertainty is the different materials that was used to cover the vent opening in the experiments. Overall, the results from the simulations of vented deflagration scenarios in the scaled warehouse geometry are in good agreement with experimental results.

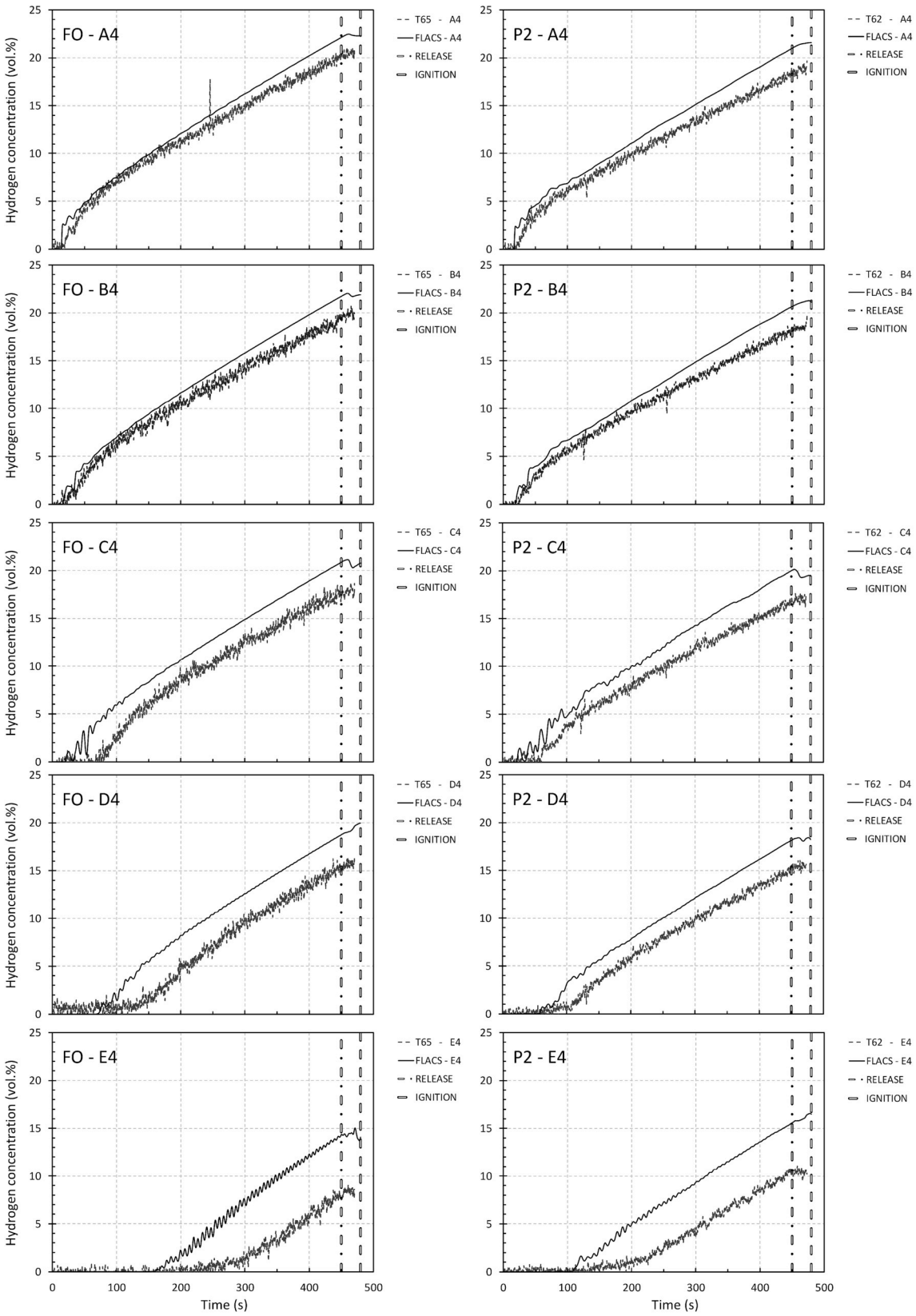

Fig. 6. Measured (dotted lines) and simulated (solid lines) hydrogen concentrations for 40 Nm^3h^{-1} jet releases with empty container (FO) and pipe rack in centre position (P2).

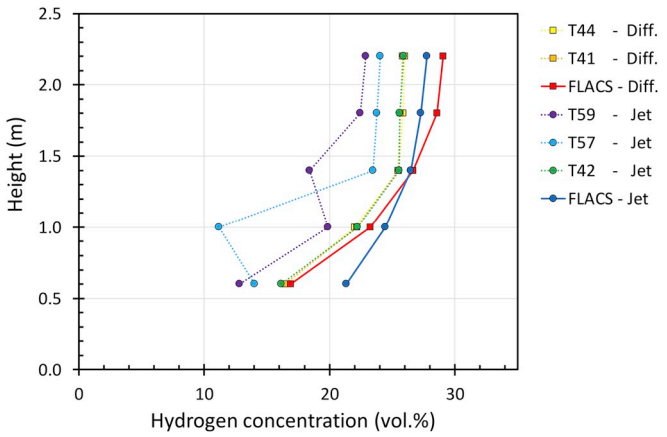

Fig. 7. Measured and simulated concentrations profiles for jet and diffusive 56 m^3h^{-1} releases in an empty container (FO).

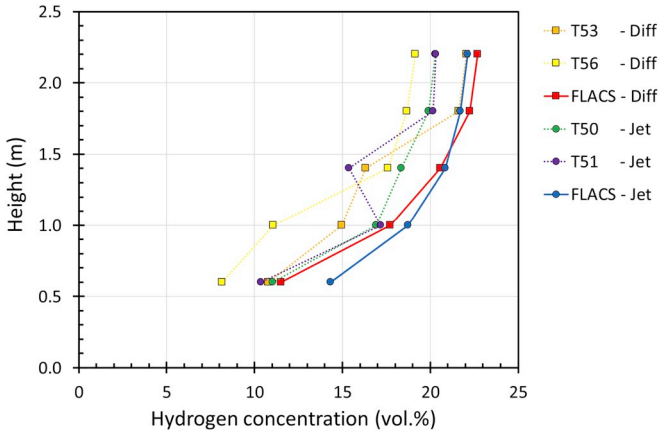

Fig. 8. Measured and simulated concentrations profiles for 42 m^3h^{-1} diffusive releases in a container with a pipe rack (P2).

4. Simulations for a realistic warehouse geometry

The results from the two validation cases presented in Section 3 indicate that FLACS-Hydrogen *v10.9* can simulate release and dispersion scenarios at moderate spatial scales with sufficient accuracy for risk assessments in industry. To this end, it is interesting to investigate relevant accident scenarios for a system that resembles an actual warehouse. Fig. 14 shows a geometry model for a hypothetical warehouse with three forklift trucks and twelve lines of pallet racking with various items. The dimensions of the warehouse are 60 m × 60 m x 9 m. The hypothetical hydrogen releases from forklift trucks in the full-scale warehouse geometry correspond to the scenarios described by Ekoto et al. (2012), but without any adjustments for spatial scale. Bauwens and Dorofeev (2014) used a geometry model for a warehouse where large, solid and smooth boxes represented entire shelves. However, this

Table 2
Test matrix and description of the test used for validation.

Test	Vent opening	Ignition location	Ignition delay (s)
T01	–	–	n/a
T02	–	–	n/a
T07	Wood screws (R1)	Near forklift (I1)	3.0
T08	Bolted wood frame (R2)	Near forklift (I1)	3.0
T12	Reinforced wood frame (R3)	Near forklift (I1)	3.0
T13	Reinforced wood frame (R3)	Ceiling (I2)	3.5

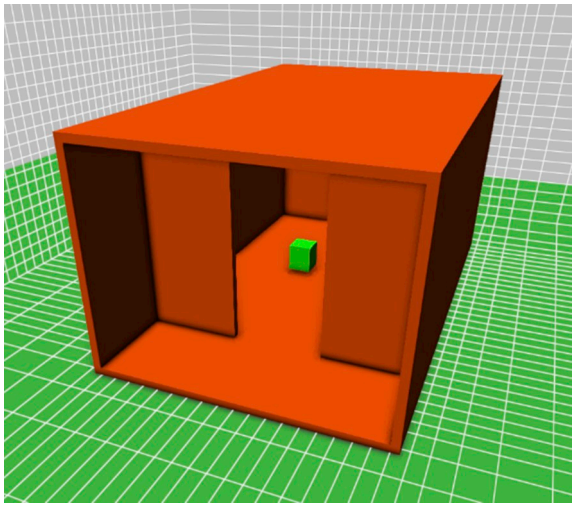

Fig. 10. Geometry model and grid for the scaled warehouse facility.

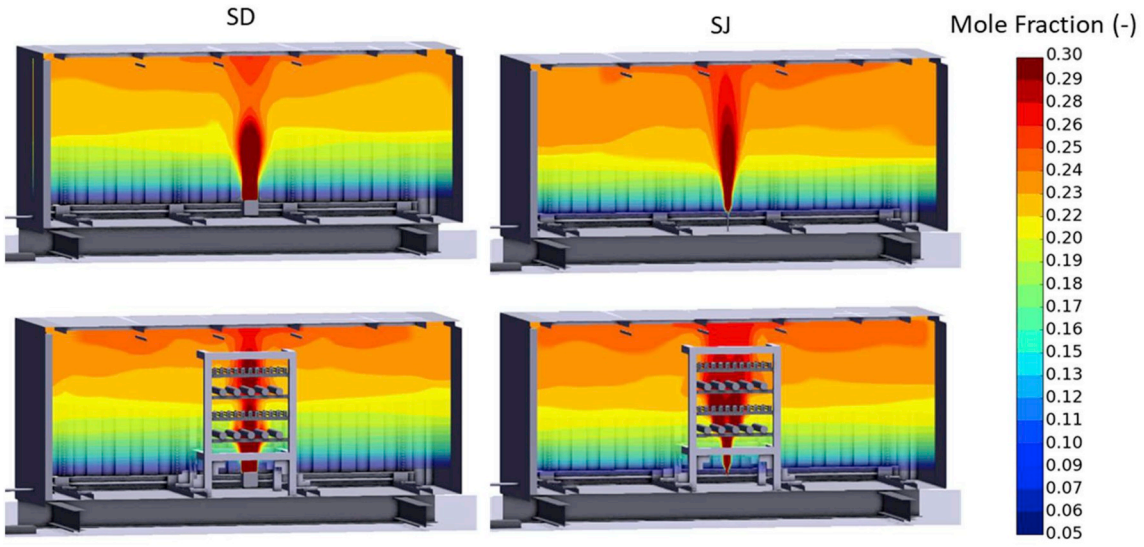

Fig. 9. Hydrogen stratification in a vertical cross-section of a container for different scenarios.

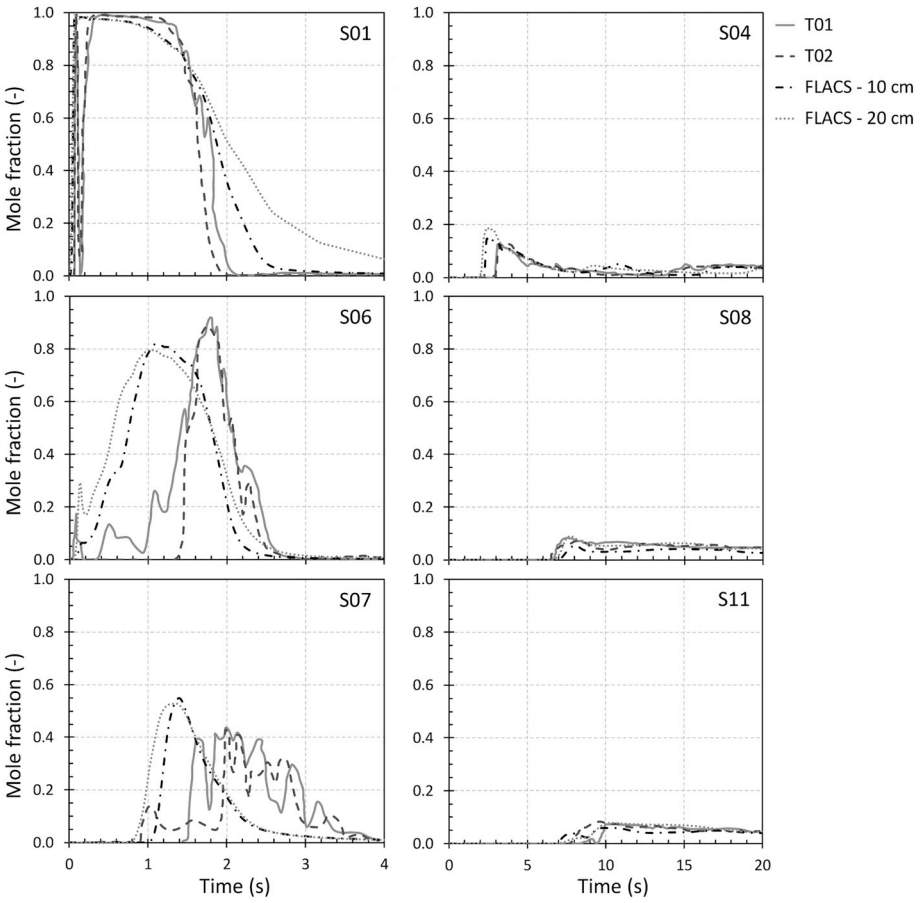

Fig. 11. Experimental and simulated hydrogen concentrations in the scaled warehouse.

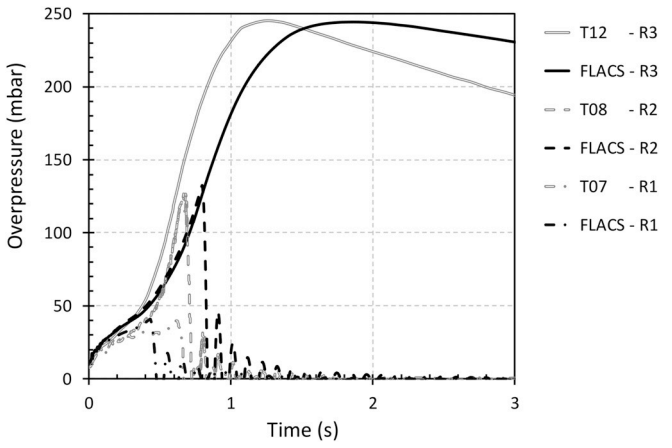

Fig. 12. Effect of reinforcing the pressure relief panels on the peak overpressure: limited reinforcement (R1), partial reinforcement (R2), and full reinforcement (R3).

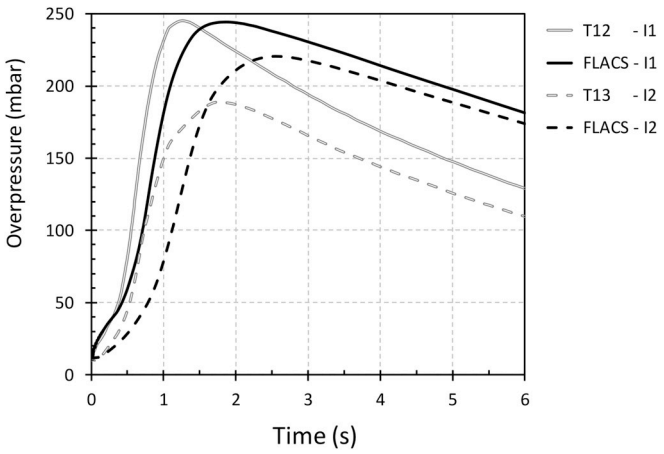

Fig. 13. Effect of ignition position on pressure development for ignition near the forklift (I1) and near the ceiling of the scaled warehouse (I2).

approach will not capture the effect of flame acceleration by congestion. Sommersel et al. (2017) demonstrated that standard size wooden pallets can cause significant flame acceleration in hydrogen-air deflagrations. The geometry model in Fig. 14 includes a relatively detailed inventory, such as boxes of different sizes and stacks of pallets in the racking. For comparison, the simulated scenarios include a geometry model where the entire pallet rackets are represented by large boxes.

The simulations used a homogeneous mesh with cubical grid cells of size 1 m. The grid was refined near the leak to a resolution of 0.13 m, in order to resolve the leaks with at least four computational cells (Gexcon, 2019). Leak files specified time-dependant flow rates consistent with the release scenarios proposed by Ekoto et al. (2012), without scaling. Fig. 15 shows selected hydrogen concentration profiles in cross-sections located at the centre of the release for different grid resolutions and different geometry configurations, 3 s after onset of the releases. Fig. 15a–c illustrate the effect of local grid refinement in the two directions normal to the release. Fig. 15d and e illustrate the hydrogen releases used for generating the initial conditions for the explosion simulations in the two geometry models.

Fig. 14. Geometry model representing a warehouse with pallet racking and three forklift trucks.

Overall, the releases in the full-scale warehouse geometry behave in the same manner as for the scaled warehouse. Refining the grid has limited effect on the hydrogen concentration 0.6 m downstream of the release point. For monitor points located about 5.2 m above the releases, the concentration decreases from 23.1 vol% to 20.6 and 9.1 vol% when the grid size in the direction of the leaks was increased from 0.15 to 0.25 and 0.50 m, respectively. Due to the limited difference in hydrogen concentration between the 0.15 and 0.25 m grid resolutions, the results from dispersion simulations on the 0.25 m grid were used as input to the explosion simulations. The CPU-time for the dispersion simulations with this grid resolution was less than 2 h. It is important that the refinement of the grid near a release point follows the same recommendations as for releases in smaller confined areas such as the scenarios presented in Chapter 3: the grid should not only be refined across the leak, but also in the direction along the leak, to resolve concentration gradients. It is also recommended to perform a grid sensitivity analysis to determine the most appropriate grid size.

Fig. 16 summarises the results from simulations of vented deflagration scenarios in two hypothetical warehouse geometries: the detailed model in Figs. 14 and 15d and the simplified model where large solid boxes represent entire pallet racks (Fig. 15e). The explosions were vented through an open door with dimensions 10 m × 7 m. The scenarios investigated assumed an accidental collision between two forklift trucks and subsequent release of the hydrogen from both trucks. The ignition location was at the front of one of the trucks. The maximum overpressures for the case with detailed inventory and grid resolutions of 0.50, 0.25 and 0.20 m are 90, 134 and 139 mbar, respectively. Hence, the results for the 0.25 and 0.20 m grid resolutions give similar values. The maximum pressure in the simplified geometry with entire rackets represented as solid boxes (simulated with a grid resolution of 0.25 m) is about 67 mbar, and the pressure decayed faster with increasing distance from the ignition point compared to the detailed model. This trend has been previously observed by Hansen et al. (2010). Fig. 15d illustrates how the flammable cloud can be partly confined between the shelves and the pallets. Flame acceleration in the stack of empty pallets resulted in the highest explosion pressures and the strongest shock wave inside the warehouse. This illustrates the importance of using a representative geometry model for consequence modelling. The effect of reducing the vent area was investigated in additional CFD simulations where the height of the open door was reduced in steps, from fully open to closed. These simulations did not result in a significant reduction in pressure. The results indicate that explosion vented devices are of limited use for warehouses of this volume and inventory of hydrogen. The situation will

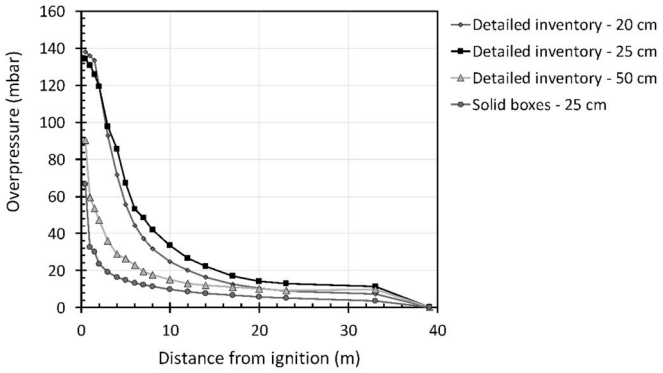

Fig. 16. Summary of results from simulations of vented deflagration scenarios in the hypothetical warehouse for different geometry models and grid resolutions.

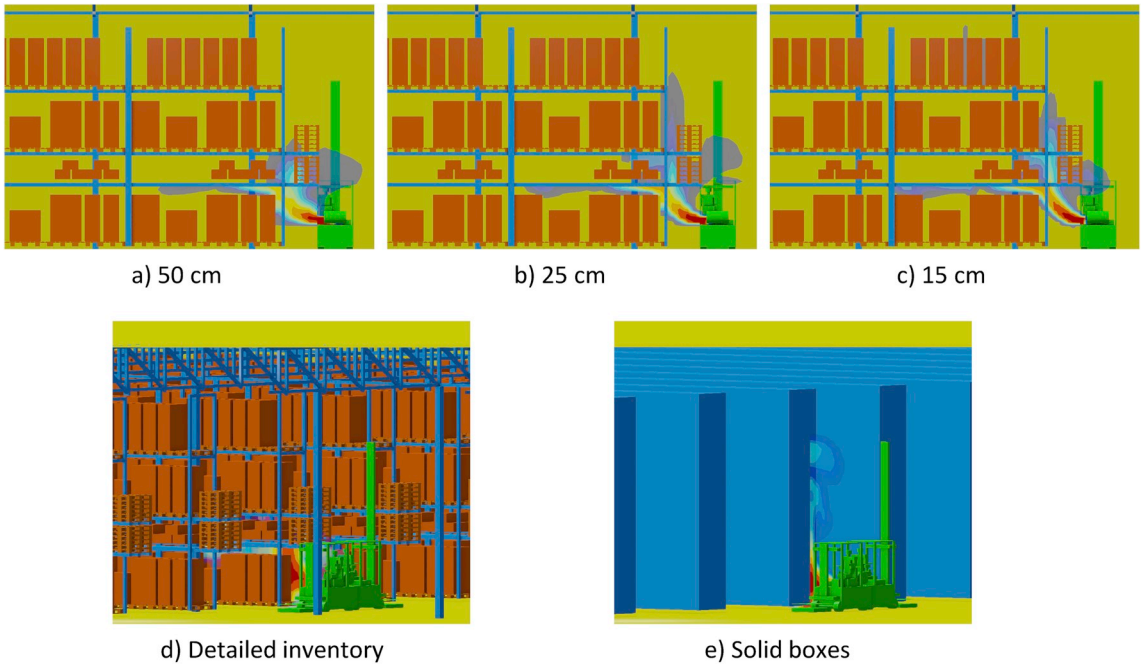

Fig. 15. Hydrogen concentration profiles in vertical cross-sections located at the centre of the releases 3 s after onset of the releases.

change for smaller warehouses and larger flammable clouds.

5. Discussion and further work

It is not feasible to perform full-scale vented deflagration experiments in realistic warehouse geometries. Hence, risk assessment for actual warehouse facilities can either rely on predictions obtained with simplified consequence models based on empirical or semi-empirical correlations, or CFD simulations. Although there is significant uncertainty associated with most model predictions (Skjold et al., 2019a), the results presented in Section 3 indicate that properly defined CFD simulations can predict the formation of stratified hydrogen-air mixtures inside enclosures with reasonable accuracy. It is also straightforward to explore the effect of natural or forced ventilation with CFD simulations.

The predictions of the flammable clouds and peak overpressures for the different scenarios illustrate the importance of using a realistic representation of the geometry in CFD simulations. Furthermore, and perhaps more importantly, the results illustrate the significant uncertainty associated with consequence modelling for industrial facilities. There is inherent uncertainty associated with the formation of explosive atmospheres, including the location of the forklift truck or trucks (leak points), the inventory of hydrogen, the flow direction and flow rate, etc. Furthermore, the consequences of vented deflagrations may vary significantly with ignition location, as well as the inventory in the pallet rackets, which is not static for a given warehouse.

For large warehouses with a limited inventory of hydrogen (e.g. the on-board capacity of a hydrogen-power forklift truck), the shock wave from a localised explosion will most likely be the primary concern with respect to the structural response of building elements. The local fuel concentration and the level and nature of the congestion within the volume occupied by the flammable cloud will probably be the controlling factors with respect to flame acceleration, and eventually the strength of the shock wave. The results from CFD simulations show that explosion venting does not represent an effective means of mitigating the effect of hydrogen explosions in large warehouses where the maximum size of a flammable cloud is determined by the inventory of hydrogen in the forklift trucks.

In principle the concerns mentioned above could be accounted for in full probabilistic risk assessments for industrial facilities. However, in practice it is not realistic to perform extensive QRAs for all warehouses, including all possible configurations of pallet rackets and inventory. A pragmatic solution can be to adopt a conservative approach based on the worst credible pressure loads resulting from flame propagation in realistic congestion. One of the features that many warehouses have in common is presumably tall stacks of empty pallets, as illustrated in Fig. 14. It should be possible to determine credible worst-case pressure loads for typical warehouses from experimental studies of flame propagation in unconfined racks filled with empty pallets. At the same time it will be possible to explore the possibility of deflagration-to-detonation-transition (DDT) for such geometries, and thereby provide input to best practice guidelines for the maximum inventory of hydrogen inside warehouses, as well as safe storage of empty pallets and other high-congestion objects in warehouses where the forklift trucks are powered by hydrogen. The results from such experiments would be highly valuable for model validation, and it may be possible to derive empirical or semi-empirical correlations for use in international standards for safe design of warehouses and similar structures where loss of containment of hydrogen represents a hazard.

6. Conclusions

This paper presents results from two validation cases where predictions obtained with the CFD tool FLACS-Hydrogen *v10.9* were compared with results from controlled experiments involving releases of compressed hydrogen and formation of stratified fuel-air clouds in confined and congested enclosures, followed by ignition and vented deflagrations. The simulations reproduced the stratification of hydrogen and the maximum reduced explosion pressures with reasonable accuracy for risk assessment purposes. The validated model system was then applied to hypothetical accident scenarios involving hydrogen releases from forklift trucks in full-scale warehouse geometries. The results demonstrate the importance of using realistic and reasonably accurate geometry models in risk assessment studies. Furthermore, the results illustrate the significant variability in the consequences of relevant scenarios that can be included in QRAs for complex systems. This highlights the importance of quantifying the uncertainty in risk assessments (Aven, 2014). Future research should explore the possibility of deriving a methodology for credible worst-case consequence assessments based on empirical data for flame propagation and pressure build-up in realistic congestion, such as pallet racks filled with empty pallets.

Acknowledgements

The HySEA project received funding from the Fuel Cells and Hydrogen 2 Joint Undertaking (FCH JU) under grant agreement No 671461. This Joint Undertaking receives support from the European Union's Horizon 2020 research and innovation programme and Hydrogen Europe and Hydrogen Europe Research.

References

Atanga, G., Lakshmipathy, S., Skjold, T., Hisken, H., Hanssen, A.G., 2019. Structural response for vented hydrogen deflagrations: coupling CFD and FE tools. Int. J. Hydrogen Energy 44, 8893–8903.
Aven, T., 2014. Risk, Surprises and Black Swans: Fundamental Ideas and Concepts in Risk Assessment and Risk Management. Routledge, New York.
Bauwens, C.R., Dorofeev, S.B., 2014. CFD modeling and consequence analysis of an accidental release in a large scale facility. Int. J. Hydrogen Energy 39, 20447–20454.
Both, A.-L., 2019. Parameter Optimisation for the Improved Modelling of Industrial-Scale Gas Explosions. PhD Thesis, University of Bergen, Norway.
Carcassi, M., Schiavetti, M., Pini, T., 2018. Non-homogeneous hydrogen deflagrations in small scale enclosure: experimental results. Int. J. Hydrogen Energy 43, 19293–19304.
Ekoto, I.W., Houf, W.G., Evans, G.H., Merilo, E.G., Groethe, M.A., 2012. Experimental investigation of hydrogen release and ignition from fuel cell powered forklifts in enclosed spaces. Int. J. Hydrogen Energy 37, 17446–17456.
EN 14994, 2007. Gas Explosion Venting Protective Systems. European Committee for Standardization (CEN), Brussels, Belgium, p. 30.
Gexcon, 2019. FLACS User's Manual v10.9. Gexcon, Bergen.
Hansen, O.R., Hinze, P., Engel, D., Davis, S., 2010. Using computational fluid dynamics (CFD) for blast wave predictions. J. Loss Prev. Process. Ind. 23, 885–906.
Hisken, H., 2018. Investigation of Instability and Turbulence Effects on Gas Explosions: Experiments and Modelling. PhD thesis, University of Bergen, Norway.
Hjertager, B.H., 1982. Simulation of transient compressible turbulent reactive flows. Combust. Sci. Technol. 27 (5–6), 159–170.
Hooker, P., Hoyes, J.R., Willoughby, D., 2017. Experimental studies of vented deflagrations in a low strength enclosure. Int. J. Hydrogen Energy 42, 7565–7576.
Houf, W.G., Evans, G.H., Ekoto, I.W., Merilo, E.G., Groethe, M.A., 2012. Hydrogen fuel-cell forklift vehicle releases in enclosed spaces. Int. J. Hydrogen Energy 38, 8179–8183.
Lakshmipathy, S., Skjold, T., Hisken, H., Atanga, G., 2019. Consequence models for vented hydrogen deflagrations: CFD vs. engineering models. Int. J. Hydrogen Energy 44, 8699–8710.
Lucas, M., Atanga, G., Hisken, H., Skjold, T., 2019. Simulating vented hydrogen deflagrations: improved modelling in the CFD tool FLACS-Hydrogen. International Conference on Hydrogen Safety (ICHS), Adelaide, 24-26 September 2019.
Makarov, D., Hooker, P., Kuznetsov, M., Molkov, V., 2018. Deflagrations of localised homogeneous and inhomogeneous hydrogen-air mixtures in enclosures. Int. J. Hydrogen Energy 43, 9848–9869.
Middha, P., 2010. Development, Use, and Validation of the CFD Tool FLACS-Hydrogen for Hydrogen Safety Studies. PhD thesis, University of Bergen, Bergen, Norway.
NFPA 68, 2018. Standard on Explosion Protection by Deflagration Venting. National Fire Protection Association (NFPA), Quincy, Massachusetts, ISBN 978-145591896-6.
Patankar, S.V., Spalding, D.B., 1972. A calculation procedure for heat, mass and momentum transfer in three-dimensional parabolic flows. Int. J. Heat Mass Transf. 15 (10), 1787–1806.
Pini, T., Hanssen, A.G., Schiavetti, M., Carcassi, M., 2019. Small scale experiments and FE model validation of structural response during hydrogen vented deflagrations. Int. J. Hydrogen Energy 44, 9063–9070.
Rao, V.C.M., Wen, J.X., 2019. Numerical modelling of vented lean hydrogen deflagrations in an ISO container. Int. J. Hydrogen Energy 44, 8767–8779.
Schiavetti, M., Pini, T., Carcassi, M., 2019. The effect of venting process on the progress of a vented deflagration. Int. J. Hydrogen Energy 44, 9080–9088.

Sinha, A., Wen, J.X., 2019. A simple model for calculating peak pressure in vented explosions of hydrogen and hydrocarbons. Int. J. Hydrogen Energy 44, 22719–22732.

Sinha, A., Rao, V.C.M., Wen, J.X., 2019a. Modular phenomenological model for vented explosions and its validation with experimental and computational results. J. Loss Prev. Process. Ind. 61, 8–23.

Sinha, A., Rao, V.C.M., Wen, J.X., 2019b. Performance evaluation of empirical models for vented lean hydrogen explosions. Int. J. Hydrogen Energy 44, 8711–8726.

Skjold, T., 2018. Vented hydrogen deflagrations in 20-foot ISO containers. Proceedings Twelfth International Symposium on Hazards, Prevention and Mitigation of Industrial Explosions (XII ISHPMIE), ISBN 978-1-5323-8443-1.

Skjold, T., 2018. Experimental investigation of vented hydrogen deflagrations in containers: homogeneous and inhomogeneous mixtures. Report 638. HySEA-D2-08-2018.

Skjold, T., Hisken, H., Bernard, L., Mauri, L., Atanga, G., Lakshmipathy, S., Lucas, M., Carcassi, M., Schiavetti, M., Rao, V.C.M., Sinha, A., Tolias, I.C., Giannissi, S.G., Venetsanos, A.G., Stewart, J.R., Hansen, O.R., Kumar, C., Krumenacker, L., Laviron, F., Jambut, R., Huser, A., 2019. Blind-prediction: estimating the consequences of vented hydrogen deflagrations for inhomogeneous mixtures in 20-foot ISO containers. J. Loss Prev. Process. Ind. 61, 220–236.

Skjold, T., Hisken, H., Lakshmipathy, S., Atanga, G., van Wingerden, M., Olsen, K.L., Holme, M.N., Turøy, N.M., Mykleby, M., van Wingerden, K., 2019. Vented hydrogen deflagrations in containers: effect of congestion for homogeneous and inhomogeneous mixtures. Int. J. Hydrogen Energy 44, 8819–8832.

Sommersel, O.K., Vaagsaether, K., Bjerketvedt, D., 2017. Hydrogen explosions in 20′ ISO container. Int. J. Hydrogen Energy 42, 7740–7748.

UN, 2018. Accelerating SDG 7 Achievement: Policy Brief 16 – Interlinkages between Energy and Transport. United Nations, p. 11, 2018.